Mechanics and Mechanical Engineering
Vol. 17, No. 2 (2013) 141–155

Stability of Thin–Walled Channel Beams with Orthotropic Flanges

Ewa Magnucka-Blandzi
Krzysztof Zając
Institute of Mathematics
Poznań University of Technology
ul. Piotrowo 3a, 60-965 Pozna, Poland
WOM Brodnica
Podgórna 90, 87-300 Brodnica, Poland
ewa.magnucka-blandzi@put.poznan.pl
k.zajac_83@poczta.onet.pl

Received (11 March 2013)
Revised (16 April 2013)
Accepted (20 May 2013)

The paper is devoted to a cold–formed, thin–walled channel beam. The appropriately shaped flanges are orthotropic structures. The mathematical model of the beam has been described. Geometrical properties of the cross section have been derived, and critical stresses of global buckling have been calculated. Two cases are considered: the problem of lateral buckling (the beam under pure bending) and the problem of global buckling (the beam under compression). The study of global buckling includes flexural and torsional buckling. The numerical model of the beam has also been formulated. The critical loads have been analytically and numerically (with the use of FEM – finite strip method) calculated. The obtained results have been compared and presented in Figures and Tables.

Keywords: Stability, thin–walled structures, numerical and analytical analysis.

1. Introduction

Cold–formed thin–walled beams are widely applied in many engineering structures – vehicles, machines, buildings and others. Thin–walled beams are at risk of losing their stability. The global buckling especially lateral buckling phenomenon as well as local buckling of beam parts play crucial role and they must not be omitted while designing process. Strength and buckling problems of these beams are described in many monographs and papers of the 20th century, for example in chronological order by Vlasov [1], Bleich [2], Timoshenko and Gere [3], Murray [4], Bažant and Cedolin [5], Weiss and Giżejowski [6], and Trahair [7].

Besides monographs, these problems have been presented in many papers for years. Rasmussen [8] presented a general bifurcation analysis of thin–walled beams.

Hancock [9] used FSM (finite strip method) to study local, distortional and flexural–torsional buckling problems of I–beams, and together with Papangelis [10] studied analytically and numerically buckling problems of thin–walled beams with open and closed cross sections. Put et al. [11, 12] concentrated with cold–formed lipped channel–section beams.

Shapes of flanges or webs of cold–formed thin–walled channel beams are rather complicated. Davis [13], Magnucki and Paczos [14] overview problems of channel beams. Selected problems of buckling and optimal design of cold–formed thin–walled beams were reviewed by Magnucka–Blandzi and Magnucki [15].

The subject of the paper is thin–walled channel beams with orthotropic flanges. The beam is compressed (Fig. 1) or in pure bending state. Flanges consist of two plates. The outer one (a top site of the flange) is a flat plate. The second one (a bottom site of the flange) is corrugated plate (a cosine wave) as it is shown in Fig. 1. Top and bottom parts of each flange are not joined together. These parts are in contact only.

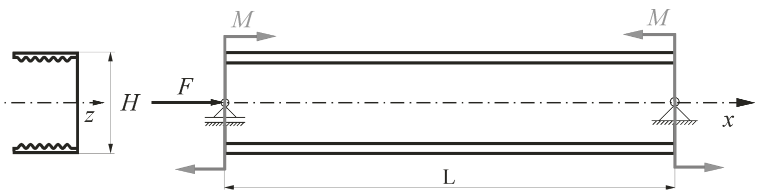

Figure 1 Scheme of simply supported thin–walled channel beam and loads

2. Geometric Properties of the Cross Section of the Beam

The cross section of the considered beam is mono–symmetrical C–section. Its scheme with principal axes yz is shown in Fig. 2. The origin $O\,(0,\,0)$ and the shear center (the point C) are located on the z–axis of symmetry.

Letter t denotes a thickness of the beam, c_a and b_0 its amplitude and period respectively, a and b dimensions of the cross section, and $H = 2a + t$ a depth of the beam.

Dimensionless parameters are

$$m \quad x_0 = \frac{b_0}{b} \quad x_1 = \frac{b_1}{b} \quad x_2 = \frac{c_a}{b} \quad x_3 = \frac{t}{b} \quad x_4 = \frac{b}{a} \tag{1}$$

A total area of the cross section is as follow

$$A = 2at\, f_0\,(x_0, x_1, x_4) \tag{2}$$

where dimensionless function is

$$f_0\,(x_0, x_1, x_4) = 1 + x_4\,(1 + 2x_1 + m x_0 S_0) \tag{3}$$

$$S_0 = \int\limits_0^1 \sqrt{1 + k^2 \sin^2(2\pi\zeta_1)}\, d\zeta_1 \quad \zeta_1 = z_1/b_0 \quad k = \pi\frac{x_2}{x_0} \tag{4}$$

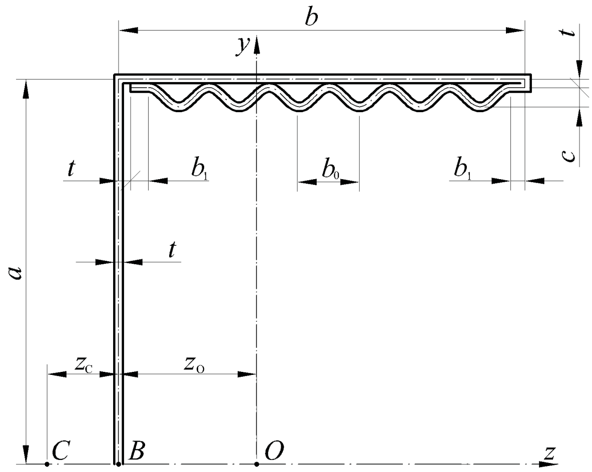

Figure 2 Scheme of the cross section of a beam with orthotropic flanges

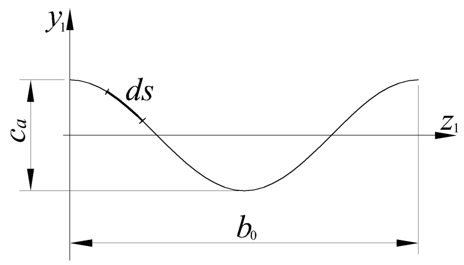

Figure 3 Scheme of a single arc

m denotes the number of cosine waves and S_0 the arc length presented in Fig. 3. The geometric stiffness for Saint–Venant torsion of the cross section is given in the formula

$$J_t = \frac{2}{3} a t^3 f_0 \left(x_0,\ x_1,\ x_3, x_4 \right) \tag{5}$$

The location of the centroid (point O) follows from a first moment of the cross section with respect to the principal axis y which equals zero, i.e.

$$z_0 A - 2t \left\{ \frac{1}{2} b^2 + b_1 \left(b + t \right) + \frac{1}{2} b_0 S_0 m \left[2 \left(b_1 + t \right) + m b_0 \right] \right\} = 0 \tag{6}$$

therefore

$$z_0 = \frac{a}{2} \frac{f_1 \left(x_0, x_1, x_3, x_4 \right)}{f_0 \left(x_0, x_1, x_4 \right)} \tag{7}$$

Moments of inertia of the plane area with respect to the y and z axes are as follows

$$J_y = 2a^3tx_4^3\left\{\frac{1}{3}+x_1\left[1-x_1+\frac{2}{3}x_1^2+x_3\left(x_1+x_3\right)\right]+mx_0^3S_3\right.$$
$$\left.+mx_0S_0\left[\frac{1}{12}x_0^2\left(4m^2-1\right)+\left(x_1+x_3\right)\left(mx_0+x_1+x_3\right)\right]\right\}-z_0^2A \qquad (8)$$

therefore

$$J_y = 2a^3t\left[f_2\left(x_0,x_1,x_3\right)-\frac{1}{4}\frac{f_1^2\left(x_0,\,x_1,\,x_3,\,x_4\right)}{f_0\left(x_0,\,x_1,x_4\right)}\right] \qquad (9)$$
$$J_z = a^3t\,f_3\left(x_1,\,x_2,\,x_3,\,x_4\right) \qquad (10)$$

The location of the shear center (the point C) is given by

$$z_C - z_B = \frac{2}{J_z}\iint_A \omega_B y\,dA \qquad (11)$$

where ω_B is the sectorial coordinate, with respect to the auxiliary point B for characteristic points of the cross section of a beam, as follows:

$$\omega_{B1}=0 \qquad \omega_{B2}=-a^2x_4 \qquad \omega_{B3}=\omega_{B2}-a^2x_3x_4=-a^2x_4\left(1+x_3\right) \qquad (12)$$
$$\omega_{B4}=\omega_{B3}+a^2x_1x_4\left(1-x_3x_4\right)=-a^2x_4\left[1+x_3-x_1\left(1-x_3x_4\right)\right]$$
$$\omega_{B5}\left(z\right)=\omega_{B4}+\omega_B\left(z\right) \qquad (13)$$
$$\omega_B\left(z\right)=a^2\left(1-x_3x_4\right)\left[2\frac{z}{a}-x_4\left(1+x_1\right)\right]-b\int_0^z x_2x_0\left(1-\cos\frac{2\pi z_0}{b_1}\right)dz_0$$
$$+a^2\left[1-x_3x_4-\frac{1}{2}x_2x_4\left(1-\cos\frac{2\pi z}{b_1}\right)\right]\left[x_4\left(1-x_1\right)-\frac{z}{a}\right] \qquad (14)$$

for $z = mbx_0$ the sectorial coordinate

$$\omega_{B5}=\omega_{B5}\left(mbx_0\right)=\omega_{B4}+a^2mx_0x_4\left[1-x_4\left(x_2+x_3\right)\right] \qquad (15)$$
$$\omega_{B6}=\omega_{B5}+a^2x_1x_4\left(1-x_3x_4\right) \qquad (16)$$

The coordinates y for characteristic points of the cross section are:

$$y_1=a \quad y_2=a \quad y_3=a\left(1-x_3x_4\right) \qquad (17)$$
$$y_4=a\left(1-x_3x_4\right) \quad y_5\left(z\right)=a\left[\left(1-x_3x_4\right)-\frac{1}{2}x_2x_4\left(1-\cos\frac{2\pi z}{x_1x_4a}\right)\right] \qquad (18)$$

for $z = mbx_0$ the coordinate $y_5 = y_5\left(mbx_0\right) = a\left(1-x_3x_4\right)$, and $y_6 = a\left(1-x_3x_4\right)$. Therefore

$$z_C - z_B = a\frac{f_4\left(x_0,x_1,x_2,x_3,x_4\right)}{f_3\left(x_0,\,x_1,\,x_2,\,x_3,\,x_4\right)} \qquad (19)$$

The sectorial coordinates (the warping functions) with respect to the shear center – point C for characteristic points of the cross section are:

$$\omega_1=\left(z_B-z_C\right)a \quad \omega_2=\omega_1-a^2x_4 \quad \omega_3=\omega_2-a^2x_3x_4\left(x_4+z_B-z_C\right) \qquad (20)$$
$$\omega_4=\omega_3+a^2x_1x_4\left(1-x_3x_4\right) \quad \omega_5\left(z\right)=\omega_4+\omega_C\left(z\right) \qquad (21)$$

where

$$\omega_C(z) = 2(a-t)z - \int\limits_0^z c_a \left[1 - \cos\left(2\pi\frac{z_0}{b_0}\right)\right] dz_0$$
$$+ \left\{a - t - \frac{1}{2}c_a\left[1 - \cos\left(2\pi\frac{z}{b_0}\right)\right]\right\}(b - b_1 - z + z_B - z_C) \tag{22}$$
$$-(a-t)(b - b_1 + z_B - z_C)$$

for $z = mbx_0$

$$\omega_5 = \omega_5(mbx_0) = \omega_4 + ma^2 x_0 x_4 [1 - x_4(x_2 + x_3)] \tag{23}$$

and

$$\omega_6 = \omega_5 + a^2 x_1 x_4 (1 - x_3 x_4) \tag{24}$$

Then the warping moment of inertia of the area of the cross section is as follows

$$J_\omega = \iint\limits_A \omega^2(s)\, dA \tag{25}$$

which is equal to

$$J_\omega = 2t(J_{\omega1} + J_{\omega2} + J_{\omega3} + J_{\omega4} + J_{\omega5} + J_{\omega6}) \tag{26}$$

where

$$J_{\omega1} = \frac{1}{3}a^3(z_B - z_C)^2 \tag{27}$$
$$J_{\omega2} = \frac{1}{3}a^2 b\left[(z_B - z_C - b)^2 + (z_B - z_C)(2z_B - 2z_C - b)\right] \tag{28}$$
$$J_{\omega3} = \frac{1}{3}t\left\{(z_B - z_C - b)^2 a^2\right.$$
$$\left.+ [(z_B - z_C)(a-t) - b(a+t)][(z_B - z_C)(2a - t) - b(2a+t)]\right\} \tag{29}$$
$$J_{\omega4} = \frac{1}{3}b_1\left\{[(b_1 + z_B - z_C)(a-t) - b(a+t)]^2\right.$$
$$\left.+ [(z_B - z_C)(a-t) - b(a+t)][(b_1 + 2z_B - 2z_C)(a-t) - 2b(a+t)]\right\} \tag{30}$$
$$J_{\omega5} = mb_0\left\{A_5^2 b_0^2 S_1 + A_1^2 b_0^2 S_4 + 2A_1 A_5 b_0^2 S_5 + 2A_4 A_5 b_0 S_6 + A_1 A_4 b_0 S_7\right.$$
$$+ A_4^2 S_8 + \left\{A_1 A_2 b_0 + A_2^2 + A_3(m-1)\left[A_2 + \frac{1}{6}A_3(2m-1) + \frac{1}{2}A_1 b_0\right]\right\} S_2$$
$$+ \left\{\frac{1}{6}A_6^2[m(2m-3)+1] + A_7^2 + A_5 A_7 b_0 + A_6(m-1)\left[A_7\right.\right.$$
$$\left.\left.\left.+ \frac{1}{2}A_5 b_0\right]\right\} S_0\right\} \tag{31}$$
$$J_{\omega6} = \frac{1}{3}b_1\left\{[(2b_1 + z_B - z_C)(a-t) - b(a+t) + mb_0(a - t - c_a)]\right.$$
$$[(3b_1 + 2z_B - 2z_C)(a-t) - 2b(a+t) + 2mb_0(a - t - c_a)]$$
$$\left.+ [(b_1 + z_B - z_C)(a-t) - b(a+t) + mb_0(a - t - c_a)]^2\right\} \tag{32}$$

3. Global Buckling

Two cases of loads are considered. The first one is a beam under pure bending (a beam carries two equal moments at its ends). In this case, the lateral buckling moment of a thin–walled beam under pure bending is as follows [6]:

$$M_{\mathrm{CR}} = \frac{\pi E}{\sqrt{2\,(1+\nu)}L}\sqrt{J_y J_t\left[1+2\,(1+\nu)\,\frac{\pi^2}{L^2}\frac{J_\omega}{J_t}\right]} \tag{33}$$

and the critical stress is given in the formula

$$\sigma_{\mathrm{CR}}^{(\mathrm{Lateral})} = \frac{M_{\mathrm{CR}}}{J_z}a \tag{34}$$

The second case is a beam subjected to a compressive force. Two global buckling modes are taking into account. The first one – flexural buckling. Then the critical force (the Euler critical force) is as follows [6]:

$$F_{\mathrm{CR}}^{(\mathrm{Euler})} = \frac{\pi^2 E J_y}{L^2} \tag{35}$$

and the critical stress can be written in the formula

$$\sigma_{\mathrm{CR}}^{(\mathrm{Euler})} = \frac{F_{\mathrm{CR}}^{(\mathrm{Euler})}}{A} \tag{36}$$

The second case of global buckling for the beam under compression is presented, that means – torsional buckling. Then the critical force (the Wagner critical force) is as follows [6]:

$$F_{\mathrm{CR}}^{(\mathrm{Wagner})} = \frac{AE}{J_y + J_z + (z_0 - z_c)^2 A}\left[\frac{J_t}{2\,(1+\nu)} + \frac{\pi^2}{L^2}J_\omega\right] \tag{37}$$

and the critical stress can be written in the formula

$$\sigma_{\mathrm{CR}}^{(\mathrm{Wagner})} = \frac{F_{\mathrm{CR}}^{(\mathrm{Wagner})}}{A} \tag{38}$$

4. Numerical Calculations

Buckling problems of thin–walled channel beams with orthotropic flange are numerically solved with the use of the finite strip method (CUFSM – B. Schafer). Obtained results are compared to analytical ones. Material constants are: the Young's modulus $E = 2 \cdot 10^5$ MPa, the Poisson's ratio $\nu = 0.3$. Horizontal axes in all figures are the relative length $\lambda = L/H$, where L is a length of beam and H is a height of the beam. Three examples are presented below. Each considered beam has the same area of a cross section and these same following dimensions: H, a, b, b_1.

4.1. *Example 1*

Detailed numerical analysis and results of analytical calculations have been conducted for the beam with following sizes: $H = 200\,\mathrm{mm}$, $m = 5$, $t = 1\,\mathrm{mm}$, $a = (H - t)/2 = 99.5\,\mathrm{mm}$, $b = 99.5\,\mathrm{mm}$, $b_1 = 11.75\,\mathrm{mm}$, $b_0 = (b - 2b_1 - t)/m = 15\,\mathrm{mm}$, $c_a = 10\,\mathrm{mm}$.

The values of critical stresses have been analytically obtained ($\sigma_{\mathrm{CR}}^{(\mathrm{Lateral})}$) based on the Eqn (34), and numerically ($\sigma_{\mathrm{CR}}^{(\mathrm{FSM})}$) with the use of FS method for lateral buckling, and have been presented in Fig. 4 and Tab. 1.

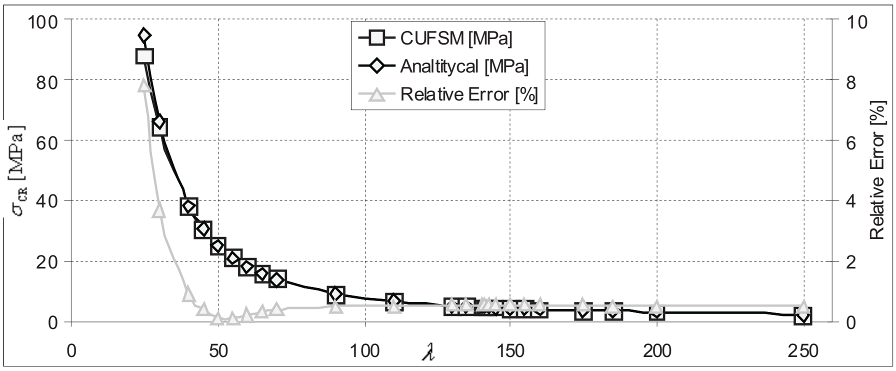

Figure 4 Comparison of analytical and numerical results – lateral buckling

Table 1 Critical stresses $\sigma_{\mathrm{CR}}^{(\mathrm{Lateral})}$ – lateral buckling

λ	25	30	40	45	50	55	60	65
$\sigma_{\mathrm{CR}}^{(\mathrm{Lateral})}$	94.64	66.30	38.11	30.50	25.05	21.01	17.94	15.54
$\sigma_{\mathrm{CR}}^{(\mathrm{FSM})}$	87.78	63.95	37.78	30.38	25.03	21.03	17.98	15.59
Relative error %	7.81	3.67	0.87	0.39	0.08	0.10	0.22	0.32
λ	70	90	110	130	145	160	175	185
$\sigma_{\mathrm{CR}}^{(\mathrm{Lateral})}$	13.63	8.89	6.45	5.01	4.28	3.73	3.31	3.08
$\sigma_{\mathrm{CR}}^{(\mathrm{FSM})}$	13.68	8.93	6.48	5.04	4.30	3.75	3.33	3.09
Relative error %	0.37	0.45	0.47	0.60	0.47	0.54	0.60	0.32

While the beam has been compressed two types of buckling mode have occurred: flexural and torsional buckling. The values of critical stresses have been analytically calculated based on Eqs. (35) and (38) respectively. Comparison of numerical and analytical results have been presented in Fig. 5 for flexural and torsional buckling modes.

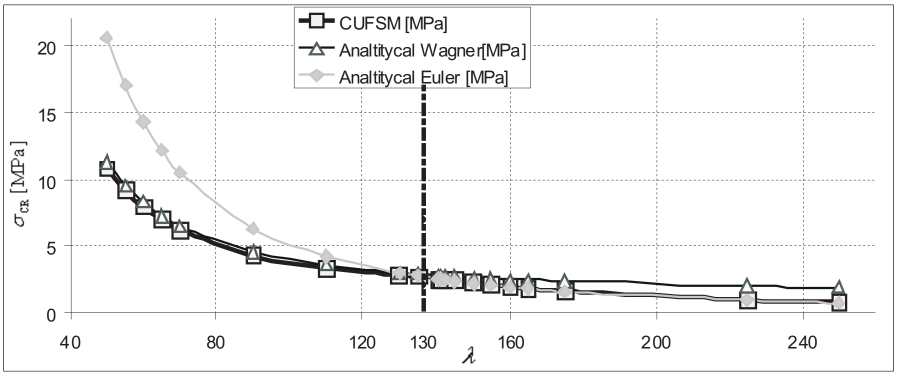

Figure 5 Comparison of analytical and numerical results for flexural and torsional buckling

In Tab. 2 and Fig. 6 comparison of analytical and numerical calculations for torsional buckling mode is only shown, and in Tab. 3 and Fig. 7 only for flexural buckling.

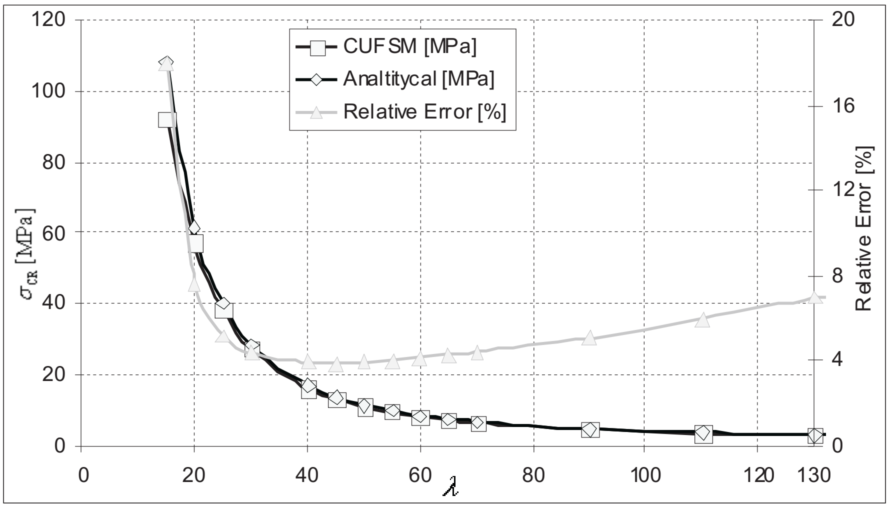

Figure 6 Comparison of analytical and numerical results for torsional buckling

Table 2 Critical stresses $\sigma_{CR}^{(Wagner)}$ – torsional buckling

λ	15	20	25	30	40	45	50
$\sigma_{CR}^{(Wagner)}$	108.43	61.70	40.07	28.32	16.64	13.48	11.23
$\sigma_{CR}^{(FSM)}$	91.89	57.33	38.12	27.15	16.01	12.98	10.8
Relative error %	18.00	7.62	5.12	4.31	3.94	3.85	3.98
λ	55	60	65	70	90	110	**130**
$\sigma_{CR}^{(Wagner)}$	9.56	8.29	7.30	6.52	4.58	3.60	**3.04**
$\sigma_{CR}^{(FSM)}$	9.19	7.96	7.01	6.25	4.36	3.4	**2.84**
Relative error %	4.03	4.15	4.14	4.32	5.05	5.88	**7.04**

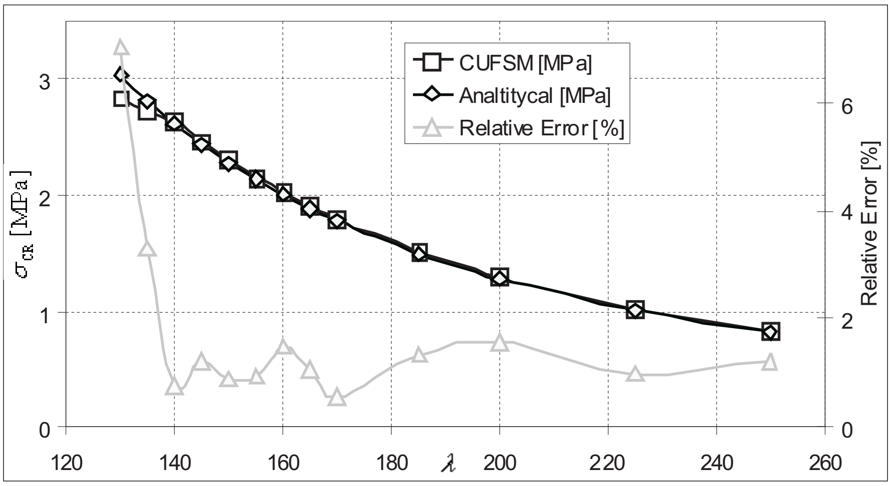

Figure 7 Comparison of analytical and numerical results for flexural buckling

Table 3 Critical stresses $\sigma_{CR}^{(Lateral)}$ – flexural buckling

λ	**130**	135	140	145	150	155	160	165	170	185	200	225	250
$\sigma_{CR}^{(Euler)}$	**3.04**	2.82	2.62	2.44	2.28	2.14	2	1.88	1.78	1.5	1.28	1.01	0.82
$\sigma_{CR}^{(FSM)}$	**2.84**	2.73	2.64	2.47	2.3	2.16	2.03	1.9	1.79	1.52	1.3	1.02	0.83
Relative error %	**7.04**	3.30	0.76	1.23	0.88	0.93	1.50	1.06	0.56	1.33	1.56	0.99	1.22

4.2. *Example 2 and 3*

Detailed numerical analysis and analytical calculations have been conducted for this same beam as in Example 1 but for a different number of cosine waves ($m = 4$ and $m = 6$), and their amplitude ($c_a = 12.5$ mm and $c_a = 8.3$ mm respectively). Considered beams have the same total area of a cross section.

The values of critical stresses in both cases for lateral buckling have been presented in Fig. 8 and Tab. 4.

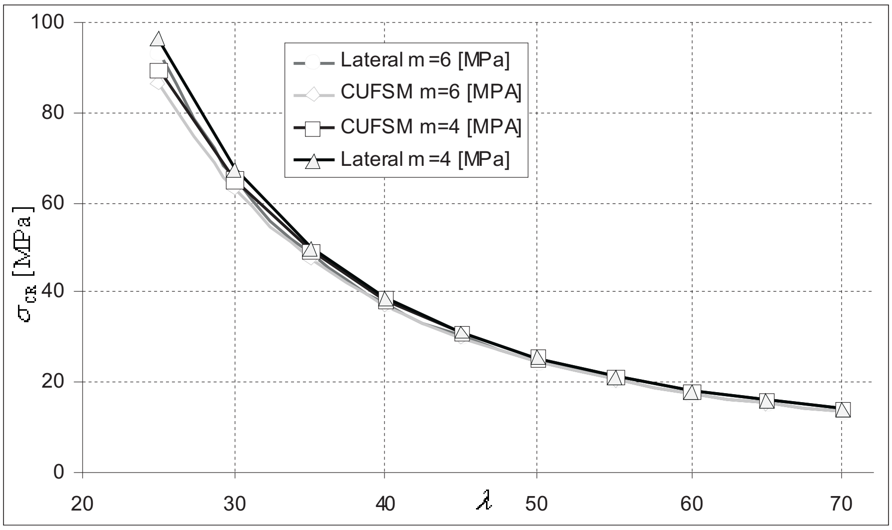

Figure 8 Comparison of analytical and numerical results – lateral buckling

Table 4 Critical stresses $\sigma_{CR}^{(Lateral)}$ – lateral buckling

λ		25	30	35	40	45	50	55	60	65	70
m=4	$\sigma_{CR}^{(Lateral)}$	96.45	67.56	50.14	38.82	31.06	25.51	21.39	18.26	15.81	13.87
	$\sigma_{CR}^{(FSM)}$	89.50	65.17	49.24	38.48	30.94	25.48	21.41	18.30	15.86	13.92
	Relative error %	7.77	3.67	1.83	0.88	0.39	0.12	0.09	0.22	0.32	0.36
m=6	$\sigma_{CR}^{(Lateral)}$	93.55	65.54	48.65	37.68	30.16	24.77	20.78	17.74	15.37	13.49
	$\sigma_{CR}^{(FSM)}$	86.74	63.22	47.78	37.35	30.04	24.75	20.80	17.78	15.42	13.54
	Relative error %	7.85	3.67	1.82	0.88	0.40	0.08	0.10	0.23	0.33	0.37

The values of critical stresses for torsional buckling, and for $m = 4$ have been presented in Fig. 9 and Tab. 5.

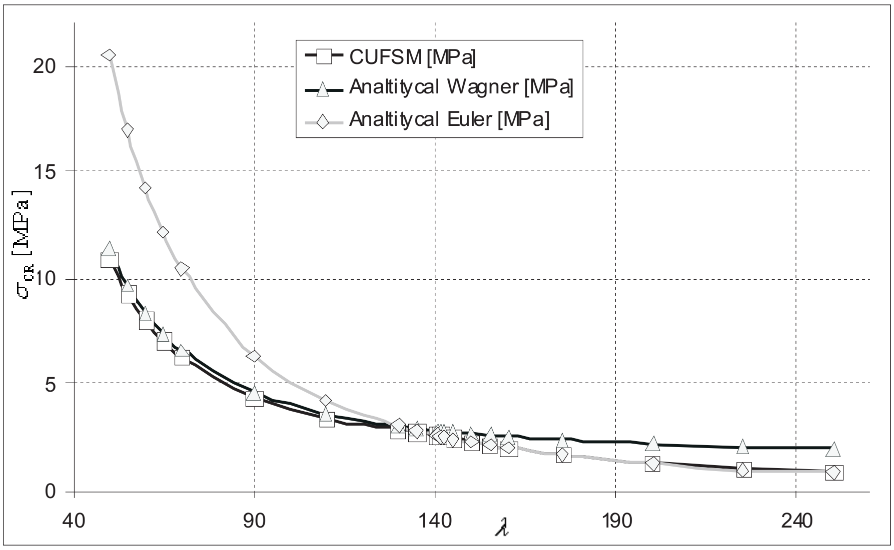

Figure 9 Comparison of analytical and numerical results for flexural and torsional buckling ($m = 4$)

Table 5 Values of critical stresses for flexural buckling ($\sigma_{\text{CR}}^{(\text{Euler})}$) and torsional buckling ($\sigma_{\text{CR}}^{(\text{Wagner})}$) for $m = 4$

λ	50	60	70	90	110	120	**130**
$\sigma_{\text{CR}}^{(\text{FSM})}$	10.89	8.02	6.28	4.38	3.41	3.09	**2.84**
$\sigma_{\text{CR}}^{(\text{Wagner})}$	11.33	8.36	6.57	4.61	3.62	3.29	**3.04**
Relative error %	4.04	4.24	4.62	5.25	6.16	6.47	**7.04**
$\sigma_{\text{CR}}^{(\text{Euler})}$	20.52	14.25	10.47	6.33	4.24	3.56	**3.04**
Relative error %	88.43	77.68	66.72	44.52	24.34	15.21	**7.04**
λ	140	150	170	200	225	250	
$\sigma_{\text{CR}}^{(\text{FSM})}$	2.64	2.31	1.79	1.30	1.02	0.83	
$\sigma_{\text{CR}}^{(\text{Wagner})}$	2.85	2.69	2.45	2.21	2.09	1.99	
Relative error %	7.95	16.45	36.87	70.00	104.90	139.76	
$\sigma_{\text{CR}}^{(\text{Euler})}$	2.62	2.28	1.77	1.28	1.01	0.82	
Relative error %	0.76	1.32	1.13	1.56	0.99	1.22	

The values of critical stresses for flexural buckling mode and for m = 6 have been presented in Fig. 10 and Tab. 6.

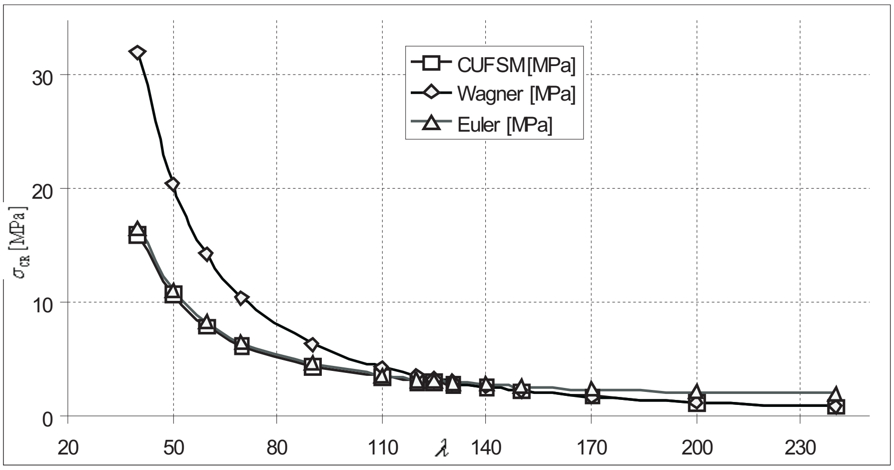

Figure 10 Comparison of analytical and numerical results for flexural and torsional buckling ($m = 6$)

Table 6 Values of critical stresses for flexural buckling ($\sigma_{\mathrm{CR}}^{(\mathrm{Euler})}$) and torsional buckling ($\sigma_{\mathrm{CR}}^{(\mathrm{Wagner})}$) for $m = 6$

λ	40	50	60	70	90	110	120
$\sigma_{\mathrm{CR}}^{(\mathrm{FSM})}$	15.95	10.77	7.94	6.23	4.36	3.40	3.09
$\sigma_{\mathrm{CR}}^{(\mathrm{Wagner})}$	16.56	11.18	8.26	6.50	4.57	3.60	3.28
Relative error %	3.82	3.81	4.03	4.33	4.82	5.88	6.15
$\sigma_{\mathrm{CR}}^{(\mathrm{Euler})}$	32.08	20.53	14.26	10.48	6.34	4.24	3.56
Relative error %	101.13	90.62	79.60	68.22	45.41	24.71	15.21
λ	125	**130**	140	150	170	200	240
$\sigma_{\mathrm{CR}}^{(\mathrm{FSM})}$	2.96	**2.84**	2.64	2.31	1.79	1.30	0.90
$\sigma_{\mathrm{CR}}^{(\mathrm{Wagner})}$	3.15	**3.03**	2.84	2.68	2.45	2.22	2.04
Relative error %	6.42	**6.69**	7.58	16.02	36.87	70.77	126.67
$\sigma_{\mathrm{CR}}^{(\mathrm{Euler})}$	3.28	**3.03**	2.62	2.28	1.78	1.28	0.89
Relative error %	10.81	**6.69**	0.76	1.32	0.56	1.56	1.12

5. Conclusions

In the paper the mathematical model of a cold–formed thin–walled channel beam with orthotropic flanges is presented. Analytical and numerical studies are devoted to global buckling. Two cases of loads are considered: the first one is the beam axially compressed and the second one the beam under pure bending. The formulas for global buckling critical loads are obtained. Numerical calculations have been performed not only using analytical formulae presented in the paper but also with the use of finite strip method. The values of critical loads obtained from each method correspond to each other very well. The change of cosine waves number does not have crucial influence for differences between analytical and numerical results. Differences decrease in lateral buckling mode for sufficiently long beams if the beam length increases. When the beam is axially compressed the influence of torsion on the buckling load may be observed for the shorter beam while the flexural buckling mode has revealed for the longer one.

References

[1] **Vlasov, V. Z.**: Thin–walled elastic bars, *Fizmatgiz*, Moscow, 1st ed. (in Russian), **1940**.

[2] **Bleich, F.**: Buckling strength of metal structures, *McGraw–Hill*, New York, **1952**.

[3] **Timoshenko, S. P. and Gere, J. M.**: Theory of elastic stability, *McGraw–Hill Book Co.*, New York, **1961**.

[4] **Murray, N. W.**: Introduction to the theory of thin–walled structures, *Clarendon Press*, Oxford, **1986**.

[5] **Bažant, Z. P. and Cedolin, L.**: Stability of structures, *Oxford University Press*, New York, Oxford, **1991**.

[6] **Weiss, S. and Giżejowski, M.**: *Stability of metal constructions*, Arkady, Warsaw, (in Polish), **1991**.

[7] **Trahair, N. S.**: Flexural–torsional buckling of structures, *F&FN Spon, an imprint of Chapman & Hall*, London, **1993**.

[8] **Rasmussen, K. J. R.**: Bifurcation of locally buckled members, *Thin–Walled Structures*, 28(2), 117–154, **1997**.

[9] **Hancock, G. J.**: Local, distortional, and lateral buckling of I–beams, *Journal of the Structural Division*, 104(11), ASCE, 1787–1798, **1978**.

[10] **Papangelis, J. P. and Hancock, G. J.**: Computer Analysis of Thin–Walled Structural Members, *Computers and Structures*, 56(1), 157–176, **1995**.

[11] **Put, B. M., Pi Youg-Lin and Trahair, N. S.**: Lateral buckling tests on cold–formed channel beams, *Journal of Structural Engineering*, 125(5), 532–539, **1999**.

[12] **Put, B. M., Pi Youg-Lin and Trahair, N. S.**: Bending and torsion of cold–formed channel beams, *Journal of Structural Engineering*, 125(5), 540–546, **1999**.

[13] **Davies, J. M.**: Recent research advances in cold–formed steel structures, *Journal of Constructional Steel Research*, 55(1–3), 267–288, **2000**.

[14] **Magnucki, K., Paczos, P.**: Theoretical shape optimization of cold–formed thin–walled channel beams with drop flanges in pure bending, *Journal of Constructional Steel Research*, 65(8–9), 1731–1737, **2009**.

[15] **Magnucka-Blandzi, E. and Magnucki, K.**: Buckling and optimal design of cold–formed thin–walled beams: Review of selected problems, *Thin–Walled Structures*, 49(5), 554–561, **2011**.

Appendix: Detailed expressions

Dimensionless functions:

$$f_1\left(x_0,x_1,x_3,x_4\right)=x_4^2\left\{1+x_1\left(2x_3+2\right)+x_0S_0\,m\left[2\left(x_1+x_3\right)+mx_0\right]\right\}$$
$$+mx_0S_0\left[\frac{1}{12}x_0^2\left(4m^2-1\right)+\left(x_1+x_3\right)\left(mx_0+x_1+x_3\right)\right]\Bigg\} \tag{39}$$

$$f_2\left(x_0,x_1,x_3,x_4\right)=x_3^4\left\{\frac{1}{3}+x_1\left[1-x_1+\frac{2}{3}x_1^2+x_3(x_1+x_3)\right]+mx_0^3S_3\right.$$
$$+mx_0S_0\left[\frac{1}{12}x_0^2(4m^2-1)+\left(x_1+x_3\right)\left(mx_0+x_1+x_3\right)\right]\Bigg\} \tag{40}$$
$$+mx_0S_0\left[\frac{1}{12}x_0^2\left(4m^2-1\right)+\left(x_1+x_3\right)\left(mx_0+x_1+x_3\right)\right]\Bigg\}$$

$$f_3\left(x_0,\,x_1,\,x_2,\,x_3,\,x_4\right)=\frac{2}{3}++2x_4\left\{\left[1+2x_1\left(1-x_3x_4\right)^2\right]\right.$$
$$+m\,x_0\left\{\frac{x_2^2x_4^2S_2}{4}+\left[1-\left(x_3x_4+\frac{1}{2}x_2x_4\right)\right]^2S_0\right\}\Bigg\} \tag{41}$$

$$f_4\left(x_0,x_1,x_2,x_3,x_4\right)=\{-1+2x_1\left(1-x_3x_4\right)\left[-2\left(1+x_3x_4\right)\right.$$
$$+\left(2x_1+mx_0\right)\left(1-x_3x_4\right)-mx_0x_2x_4]+mx_0\left\{\left[-\left(1+x_3x_4\right)\right.\right.$$
$$-\tfrac{1}{2}x_2x_4+x_1\left(1+\tfrac{1}{2}x_2x_4-x_3x_4\right)+\tfrac{1}{2}mx_0\left(1-\tfrac{1}{2}x_2x_4-x_3x_4\right)\Big]$$
$$(2-x_2x_4-2x_3x_4)S_0+\tfrac{1}{4}(x_2x_4)^3(2-2x_1-mx_0)S_0\Big\}\Big\}\,x_4^2 \tag{42}$$

Non–elementary integrals:

$$S_1=\int_0^1\zeta^2\sqrt{1+k^2\sin^2\left(2\pi\zeta\right)}\,d\zeta \tag{43}$$

$$S_2=\int_0^1\cos^2\left(2\pi\zeta_1\right)\sqrt{1+k^2\sin^2\left(2\pi\zeta_1\right)}\,d\zeta_1 \tag{44}$$

$$S_3=2\int_0^{\frac{1}{2}}\zeta_1^2\sqrt{1+k^2\sin^2\left(2\pi\zeta_1\right)}\,d\zeta_1 \tag{45}$$

$$S_4=\int_0^1\zeta^2\cos^2\left(2\pi\zeta\right)\sqrt{1+k^2\sin^2\left(2\pi\zeta\right)}\,d\zeta \tag{46}$$

$$S_5=\int_0^1\zeta^2\cos\left(2\pi\zeta\right)\sqrt{1+k^2\sin^2\left(2\pi\zeta\right)}\,d\zeta \tag{47}$$

$$S_6 = \int_0^1 \zeta \sin(2\pi\zeta) \sqrt{1 + k^2 \sin^2(2\pi\zeta)}\, d\zeta \tag{48}$$

$$S_7 = \int_0^1 \zeta \sin(4\pi\zeta) \sqrt{1 + k^2 \sin^2(2\pi\zeta)}\, d\zeta \tag{49}$$

$$S_8 = \int_0^1 \sin^2(2\pi\zeta) \sqrt{1 + k^2 \sin^2(2\pi\zeta)}\, d\zeta \tag{50}$$

Constants:

$$A_1 = -\frac{1}{2}c_a, \quad A_2 = \frac{1}{2}c_a\left(b - b_1 + z_B - z_C\right), \quad A_3 = -\frac{1}{2}c_a b_0 \tag{51}$$

$$A_4 = \frac{1}{2\pi}c_a b_0, \quad A_5 = a - t - \frac{1}{2}c_a, \quad A_6 = \frac{1}{2}b_0\ \left(2a - 2t - c_a\right) \tag{52}$$

$$\begin{aligned} A_7 = &-\frac{1}{2}\left[2a\left(b - b_1 - z_B + z_C\right) + b_1\left(2t - c_a\right)\right. \\ &\left. + \left(c_a + 2t\right)\left(b + z_B - z_C\right)\right] \end{aligned} \tag{53}$$